



Morphology of strained and relaxed SiGe layers grown on high-index Si substrates

Morgan E. Ware^{a,*}, Robert J. Nemanich^b

^a Department of Physics, University of Arkansas, Fayetteville AR 72701, USA

^b Department of Physics, Arizona State University, Tempe AZ 85287-1504, USA

ARTICLE INFO

Article history:

Received 27 November 2008

Received in revised form 27 July 2009

Accepted 29 July 2009

Available online 7 August 2009

Keywords:

Stress

Atomic force microscopy (AFM)

Germanium

Surface morphology

Molecular beam epitaxy

ABSTRACT

We have investigated the surface morphology of strained and relaxed SiGe layers grown on Si substrates with surface normals rotated off of the [001] axis towards [111] by 0, 13, and 25°. Atomic force microscopy has revealed surface corrugations in thin layers prior to plastic relaxation on each of the surfaces due to the initial deposition of the strained films. Thicker partially relaxed layers have previously been shown to contain networks of misfit dislocations which create patterns that are unique to each substrate orientation. We find on these relaxed layers that the surface corrugations are well aligned with the dislocation networks forming a modified crosshatch pattern on the off-axis substrates. More strikingly, though, we find that these corrugations are comprised of smaller nanostructured features which are also unique to each surface. Topographs of the unrelaxed surfaces show no such organization indicating a correspondence between the misfit dislocations and the surface corrugations.

© 2009 Elsevier B.V. All rights reserved.

1. Introduction

Technological advancements using strictly Si devices are beginning to push fundamental limits of physics. SiGe based heterostructures offer possible alternatives with strain based engineering, and self-assembled nanostructures [1–3]. In particular, it has been demonstrated that strained growth on high-index substrates has the potential to controllably modify the classical self-assembly processes in semiconductor epitaxy [4–6]. In order to take advantage of properties of any such structures, it must be understood how these strained films grow and relax. A significant amount of work exists in the literature which documents the low-index surfaces of Si, i.e., (001), (110), and (111), and growth on those surfaces. However, the atomically clean high-index Si surfaces in the family between (001) and (110) are becoming more extensively characterized and understood [7,8], and knowledge of thin film growth on these substrates will further their possible use in device fabrication.

Several reviews exist which cover the current progress in SiGe growth on Si substrates and discuss the various processes by which the growth proceeds [9–11]. Among these are processes which result in a critical thickness for relaxation, either partially through the Stranski–Krastinov (SK) driven formation of islands or other nanostructures [12], or more completely through the plastic deformation of the interface by the formation of misfit dislocations [13]. Between these two extremes there also exists the possibility that the strain may drive an Asaro–Tiller–Grinfeld (ATG) instability forming an increasing surface ripple which can locally decrease strain [14,15]. These various

relaxation mechanisms are inherently interrelated [16,17] favoring one or the other depending on the total lattice mismatch between layers. For Ge growth on Si, with a relatively large mismatch of 4.2%, SK growth will result in islands forming after ~3 ML are deposited [18]. In our study, we wish to examine pseudomorphically strained layers and their subsequent relaxation by misfit dislocation formation, therefore a smaller mismatch is used by depositing a SiGe alloy with a moderate Ge content.

Growth of SiGe on Si(001) has been extensively studied. The “crosshatch” pattern resulting from strain relief has become ubiquitous, although, still not completely understood [19]. The common manifestation of this crosshatch is on (001) growth and is found to be two orthogonal arrays of surface undulations. These undulations are believed to be caused in part by the underlying misfit dislocations, each creating a monolayer step on the surface, followed by surface mass transport which acts to smooth the stepped surface into undulations [17]. Increasingly, the study of strained growth on vicinal substrates is revealing a more complex pattern of surface undulations. Giannakopoulos and Goodhew [20] have found that for InGaAs growth on (001) GaAs substrates miscut 3° from the $\bar{1}10$ direction that one of the orthogonal arrays appears as two new arrays oriented only 2–3° from parallel to each other. Other groups [21,22] have found that for strained HgCdTe deposition on the (211) substrate face these two new arrays appeared again separated by a much wider angle. In a previous study of strain-relaxed high-index samples [23] we found that relaxation of SiGe films grown on the low symmetry Si substrates oriented between (001) and (110) proceeds by forming networks of dislocations in similar patterns to the surface ripples being discovered on vicinal growth in other material systems. In this article we will examine the surface morphology resulting from this network of

* Corresponding author.

E-mail address: meware@uark.edu (M.E. Ware).

dislocations in off-axis SiGe strained growth and relaxation and compare it to the surface morphology of thin strained layers.

2. Experimental details

Commercially prepared Si substrates were obtained from Virginia Semiconductor, Fredericksburg, Virginia, USA with surface orientations off-axis from (001) to (111) by 0, 13 and 25°. These closely correspond to the (001), (116), and (113) surfaces of which only the (116) surface is not known to be stable. The substrates were subjected to a wet chemical clean for approximately 60 s using a 10:1 hydrofluoric acid solution diluted in de-ionized water. Following loading into the ultra-high vacuum (UHV) system with base pressures in the 10^{-8} Pa range, the substrates were submitted to a thermal treatment at 950 °C for 10 min to desorb any residual contaminants. After cooling to 550 °C, and immediately prior to deposition of the experimental layer, a 20 nm Si buffer layer was deposited. Auger electron spectroscopy (AES) and low energy electron diffraction (LEED) were used on a sacrificial substrate after deposition of the buffer layer to characterize the surface. The AES showed only Si to within its sensitivity, and the LEED showed a sharp $(2 \times 1) + (1 \times 2)$ reconstruction on the (001) substrates. The off-axis surfaces showed sharp LEED patterns as well, indicating atomically clean surfaces.

Immediately following the buffer layer deposition the hetero-epitaxial layers were formed by co-depositing Si and Ge in the UHV solid source molecular beam epitaxy at a substrate temperature of 550 °C and a combined rate of 0.04 nm/s. Layers of $\text{Si}_{1-x}\text{Ge}_x$, $x = 0.3$, were grown to 10 and 100 nm on each of the three differently oriented substrates. The deposition was controlled and monitored with dual 6 Mhz gold-coated quartz oscillators, which have been calibrated by profilometry. Atomic force microscopy (AFM) was performed in air using a Park Scientific Instruments model M5 in contact mode with a SiN tip to analyze the surface morphologies.

3. Results

The results of a Raman analysis, published separately [24], demonstrate clearly that the 100 nm films are significantly more relaxed than the 10 nm films. This is indicative of plastic relaxation through misfit dislocation formation which has been confirmed by transmission electron microscopy in similar 100 nm films as described in our previous study [23].

Shown in Fig. 1 are AFM images of the 10 nm films. Well defined structures are evident on all three substrate orientations, but the structures noticeably differ between substrates. The (001) surface, seen in Fig. 1a, is characterized by a rectangular based, hut-like structure which is elongated in the [100] and [010] directions. These huts have been well characterized [25], and are known to be bound by {105} facets.

The 13, and 25° off-axis surfaces, Fig. 1b and c, consists of ridges and trenches respectively aligned predominantly down in the image. Interestingly, these ridges and trenches are aligned perpendicular to the steps which form on clean Si substrates of these orientations [7].

Fig. 2 shows the topography of the 100 nm, relaxed samples. The most noticeable feature of these samples is found in the large scale, Fig. 2a,b, and c, where lines of corrugation form on the surface in very distinct patterns. All surfaces have these lines running nominally in the $[\bar{1}10]$ direction, which is to the right in the figure and is the only direction common to all three surfaces. The (001) surface, in addition, has lines running in the [110] direction completing the common crosshatch configuration. On the 13°, and 25° off-axis surfaces, though, this second set of lines appears to have split into pairs which intersect and are symmetric around the surface [110] direction similar to those Martinka et. al., found for HgCdTe/CdZnTe deposition on the (221) crystal plane [21]. These lines do not appear in any way on the 10 nm, strained surfaces. The angles at which these lines intersect have been measured to be 15.5 and 33.5° for the 13, and 25° off-axis surfaces respectively which is in complete register with the underlying misfit dislocations [23].

In addition to the large-scale organization of the relaxed surfaces we see, in Fig. 2d,e, and f, well resolved nanostructures, which are unique to each surface. These features appear as follows: rectangular huts on (001), elongated pyramids on 13° off-axis, and wide planar regions separated by low amplitude ripples on the 25° off-axis surface. In all cases these nanostructures resemble the structures found on the surface of the strained samples in Fig. 1, roughly in size and shape. For the (001) surface, the comparison is obvious with rectangular huts aligned in the [100] and [010] direction with only a reduction in size by a factor of ~ 2 . For the 13° off-axis surface, we can see that several of the elongated ridges on the strained surface, Fig. 1b, have already formed the elongated pyramidal structures. These are very similar to those found on the relaxed surface of the same orientation, Fig. 2e. The similarities between the strained and relaxed surfaces of the 25° off-axis samples are slightly more subtle, but we suggest that the planar regions are simply separated by deep trenches on the strained surface, Fig. 1c, which have filled during growth to form low amplitude ripples on the relaxed surface, Fig. 2f.

4. Discussion

The morphology of the thin strained films can be understood partially in terms of the ATG instability [14,15] by which the rippling or corrugation of the surface is a result of coherent strain elastically driving an unstable “seed” ripple into large-scale deformations of the surface. This happens without the plastic relaxation of the film and should not be considered islanding due to its continuous nature, but it does provide partial relaxation [26,27]. We have found our 10 nm

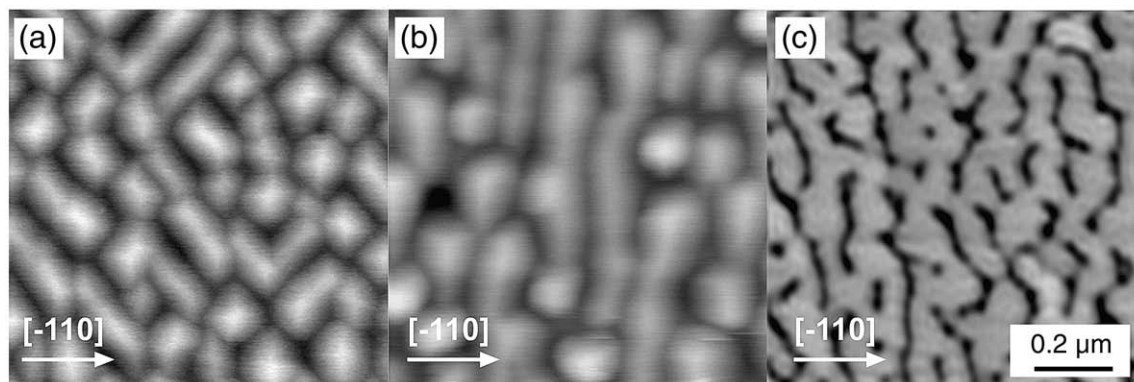


Fig. 1. AFM micrographs of 10 nm thick films of $\text{Si}_{0.7}\text{Ge}_{0.3}$ grown on (a) Si(001), (b) 13° off-axis, (c) and 25° off-axis. Average peak to valley values for (a) and (b) are ~ 10 nm indicating near three dimensional growth. The average depth of a trench in (c) is ~ 6 to ~ 8 nm. For all images the $[\bar{1}10]$ direction is to the right.

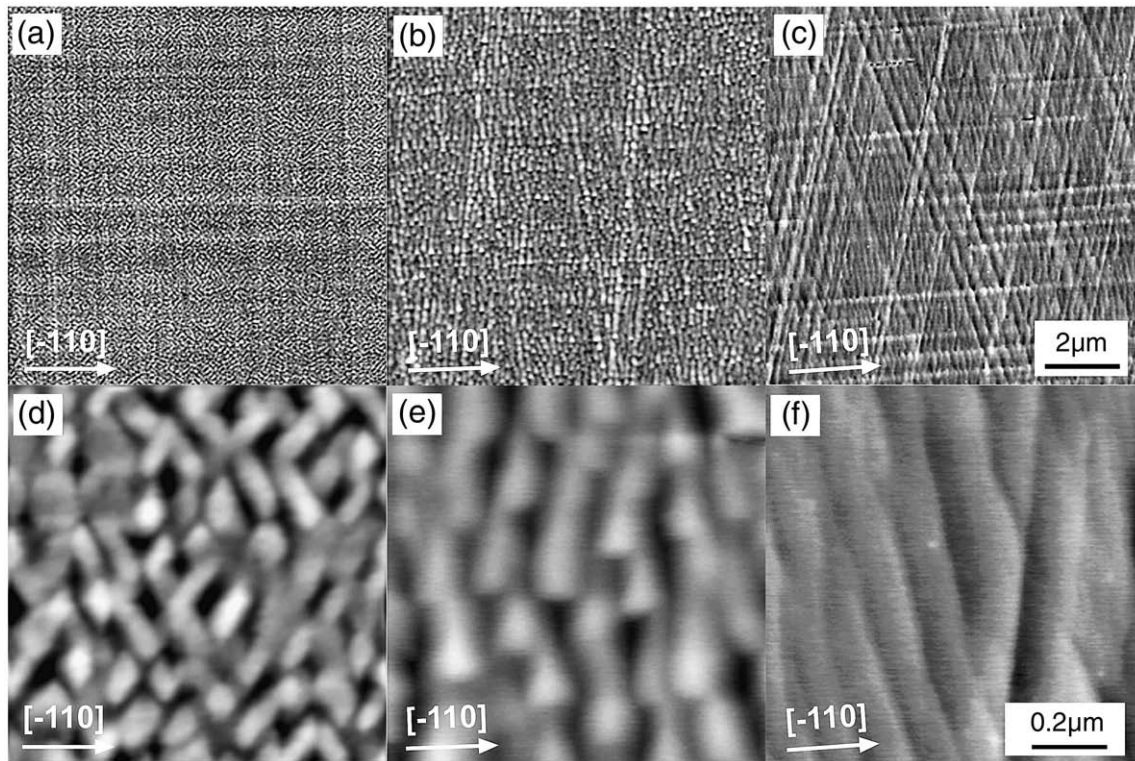


Fig. 2. AFM micrographs of 100 nm thick films of $\text{Si}_{0.7}\text{Ge}_{0.3}$ grown on (a) and (d) Si(001), (b) and (e) 13° off-axis, and (c) and (f) 25° off-axis. Images on the same substrate are different magnifications of the same sample to show different features. Average peak to valley values for all images except (c) and (f) are ~ 5 nm. (c) and (f) have average peak to valley values of ~ 2 nm. For all images the $[\bar{1}10]$ direction is to the right.

films to be free of misfit dislocations [23] indicating that this mechanism is most likely driving the surface undulation.

The hut-like structures which form on the (001) surface, seen in Fig. 1a, have been reported frequently in the literature for these conditions [28]. The irregular extended ridges seen on the 13° off-axis surface in Fig. 1b appear to be a kinetically limited formation, i.e., they were frozen into the crystal upon quenching to room temperature. Similar ridge formations have been reported by Berbezier et al. [6,29], for 10° off-axis substrates. They were shown to make a transition to regularly shaped extended pyramids, similar to those found in our relaxed samples, Fig. 2e, after several hours of annealing at the growth temperature and without dislocation formation. These extended pyramidal shapes have also been observed for strained SiGe growth on 4° off-axis Si substrates [30,31] and were found to be highly dependent on the growth temperature. We expect that the formations on our 13° off-axis strained surface would respond similarly to long anneal times.

Growth on the 25° off-axis substrate has only limited representation in the literature. Pure Ge growth on the (113) surface of Si at 25.2° off-axis has been demonstrated to form short Ge nanowires in the $[3\bar{3}\bar{2}]$ direction [32]. Compared to Fig. 1c the $[3\bar{3}\bar{2}]$ direction would be towards the bottom of the page in which there is initial evidence of alignment. This alignment indicates an anisotropy on this surface similar to the 13° off-axis surface, and it is possible that the 25° surface in our study has not reached its thermodynamic equilibrium similar to our 13° sample. Here an extended anneal at the growth temperature as in [29] might produce wire-like structures as are found for Ge deposition on the (113).

The 100 nm thick, relaxed layers, shown in Fig. 2, are characterized by their crosshatch or modified crosshatch morphology in which one direction of the cross now appears as two lines intersecting at an angle determined by the substrate orientation. It is generally accepted that the classical crosshatch feature of strain-relaxed heterostructures is caused by the misfit dislocations which provide the bulk of the relaxation [17,19,21,33–35]. We can show as a confirmation of this,

that the surface crosshatch morphology of our off-axis structures is in direct correlation with the misfit dislocations which run along the intersection of the (111) planes and the substrate surface. The angle, ϕ , at which these dislocations intersect for a substrate miscut off (001) towards $[110]$ by θ is given by [23]

$$\cos(\phi) = \frac{2 + \tan(\theta)^2}{2 + 3 \tan(\theta)^2} \quad (1)$$

Fig. 3 shows a plot of this relation, and the relative values for ϕ as measured from Fig. 2b and c. Extremely good agreement is found, and

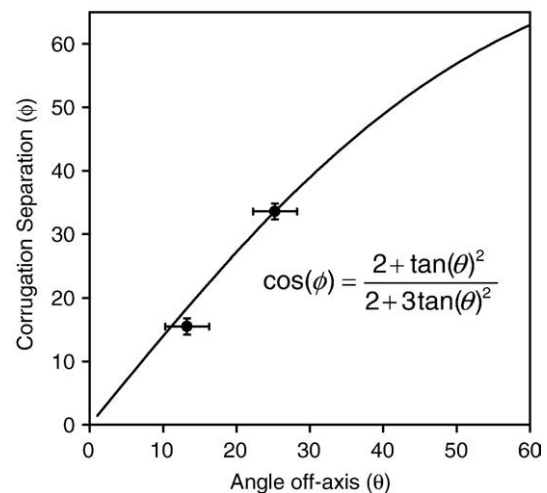


Fig. 3. Plot showing the angle of intersection, ϕ , of the $(\bar{1}11)$ and $(1\bar{1}1)$ planes within the surface for the family of substrates off-axis from (001) towards (111) by some angle, θ , given by the inset equation. The two plotted points are average values of the separation in the corrugation directions taken from the AFM images in Fig. 2.

we attribute any disagreement to uncertainty in the substrate orientation.

Further investigation of the kinetics of formation for these surfaces could be informative. There are very obvious similarities in Fig. 2a,b, and c in that they all have a form of the crosshatch pattern. However, there are dramatic differences found upon closer examination. In Fig. 2c we find a continuously sloping surface with little indication of surface structure except for the crosshatch. However, in Fig. 2a and b there are considerable surface features in addition to the crosshatch. For the (001), on-axis growth in Fig. 2a, the hut-shaped formations appear to have formed before the crosshatch, Fig. 1a, and are subsequently modulated by the formation of each line of the crosshatch. In contrast, the nanostructures forming on the 13° off-axis surface are obviously well aligned along the lines of the crosshatch with no apparent height modulation. This demonstrates a possible method for creating unique patterns of self-aligned nanostructures by which a lattice of dislocations forms a template on the surface subsequently acting as nucleation sites for the organized deposition of quantum structures. This has been demonstrated for growth on the (001) surface [36–38], and we expect should easily generalize to other surfaces.

5. Summary

We have observed the surfaces of strained and relaxed Si_{0.7}Ge_{0.3} films grown on Si substrates rotated off-axis from (001) to (111) by 0, 13, and 25°. It is found that the morphology of these surfaces undergoes a dramatic transition upon plastic relaxation. For the strained films we find characteristic features on each of the surfaces which are as follows: huts on the (001) surface, elongated pyramids on the 13° off-axis surface, and elongated ridges on the 25° off-axis surface. Upon plastic relaxation we find modified crosshatch patterns on the surfaces which are in complete registry with the underlying lattice of misfit dislocations. Of particular interest, we find on the 13° off-axis sample that the surface structures have ordered themselves with the lines of the crosshatch and without considerable undulation of the underlying surface as is found in the on-axis, (001) growth. These results should provide a starting point for the study of almost arbitrarily organized nanostructures based on a wide range of substrate orientations.

Acknowledgement

The experimental measurements reported here were completed at North Carolina State University. This research is supported by the National Science Foundation through Grants No. DMR-0512591 and DMR-0080016.

References

- [1] J.C. Bean, Proc. IEEE 80 (1992) 571.
- [2] C.K. Maiti, Semicond. Sci. Technol. 13 (1998) 1225.
- [3] K.L. Wang, S.G. Thomas, M. Tanner, J. Mater. Sci. 6 (1995) 311.
- [4] L. Fitting, M.E. Ware, J.R. Haywood, J.J.H. Walter, R.J. Nemanich, J. Appl. Phys. 98 (2005) 024317.
- [5] P.M. Lytvyn, V.V. Strelchuk, O.F. Kolomys, I.V. Prokopenko, M.Ya. Valakh, Yu.I. Mazur, Zh.M. Wang, G.J. Salamo, M. Hanke, Appl. Phys. Lett. 91 (2007) 173118.
- [6] I. Berbezier, A. Ronda, Phys. Rev., B 75 (2007) 195407.
- [7] A.A. Baski, S.C. Erwin, L.J. Whitman, Surf. Sci. 392 (1997) 69.
- [8] H.-C. Jeong, E.D. Williams, Surf. Sci. Rep. 34 (1999) 171.
- [9] I. Berbezier, A. Ronda, A. Portavoce, J. Phys. Condens. Matter (2002) 8283.
- [10] C. Teichert, Phys. Rep. 365 (2002) 335.
- [11] J. Stangl, V. Holy, G. Bauer, Rev. Mod. Phys. 76 (2004) 725.
- [12] I.N. Stranski, L. Krastanow, Akad. Wiss. Lit. Wien Math.-Natur. IIb 146 (1938) 797.
- [13] J.W. Matthews, A.E. Blakeslee, J. Cryst. Growth 27 (1974) 118.
- [14] R.J. Asaro, W.A. Tiller, Metall. Trans. 3 (1972) 1789.
- [15] M.A. Grinfeld, Sov. Phys. Dokl. 31 (1987) 831.
- [16] H. Gao, W.D. Nix, Annu. Rev. Mater. Sci. 29 (1999) 173.
- [17] A.M. Andrews, A.E. Romanov, J.S. Speck, M. Bobeth, W. Pompe, Appl. Phys. Lett. 77 (2000) 3740.
- [18] D.E. Savage, F. Liu, V. Zielasek, M.G. Lagally, in: R. Hull, J.C. Bean (Eds.), Fundamental Mechanisms of Film Growth, in Germanium Silicon: Growth and Materials, Semiconductor and Semimetals, vol. 56, Academic Press, New York, 1999, p. 49.
- [19] A.M. Andrews, J.S. Speck, A.E. Romanov, M. Bobeth, W. Pompe, J. Appl. Phys. 91 (2002) 1933.
- [20] K.P. Giannakopoulos, P.J. Goodhew, J. Cryst. Growth 188 (1998) 26.
- [21] M. Martinka, L.A. Almeida, J.D. Benson, J.H. Dinan, J. Electron. Mater. 30 (2001) 632.
- [22] J.D. Benson, L.A. Almeida, M.W. Carmody, D.D. Edwall, J.K. Markunas, R.N. Jacobs, M. Martinka, U. Lee, J. Electron. Mater. 36 (2007) 949.
- [23] M.E. Ware, R.J. Nemanich, J.L. Gray, R. Hull, J. Appl. Phys. 95 (2004) 115.
- [24] Morgan E. Ware, Ph. D. thesis, North Carolina State University, 2002.
- [25] Y.-W. Mo, D.E. Savage, B.S. Swartzentruber, M.G. Lagally, Phys. Rev. Lett. 65 (1990) 1020.
- [26] D.J. Srolovitz, Acta Metall. 37 (1989) 621.
- [27] R. Hull, J. Gray, C.C. Wu, S. Atha, J.A. Floro, J. Phys. Condens. Matter 14 (2002) 12829.
- [28] D.E. Jesson, K.M. Chen, S.J. Pennycook, T. Thundat, R.J. Warmack, Phys. Rev. Lett. 77 (1996) 1330.
- [29] I. Berbezier, M. Abdallah, A. Ronda, G. Bremond, Mater. Sci. Eng., B. 69/70 (2000) 367.
- [30] C. Teichert, J.C. Bean, M.G. Lagally, Appl. Phys. A 67 (1998) 675.
- [31] H. Lichtenberger, M. Mühlberger, F. Schäffler, Appl. Phys. Lett. 86 (2005) 131919.
- [32] H. Omi, T. Ogino, Appl. Phys. Lett. 71 (1997) 2163.
- [33] K.H. Chang, R. Gibala, D.J. Srolovitz, P.K. Bhattacharya, J.F. Mansfield, J. Appl. Phys. 67 (1990) 4093.
- [34] M.A. Lutz, R.M. Feenstra, F.K. LeGoues, P.M. Mooney, J.O. Chu, Appl. Phys. Lett. 66 (1995) 6.
- [35] R. Beanland, M. Aindow, T.B. Joyce, P. Kidd, M. Lourenço, P.J. Goodhew, J. Cryst. Growth 149 (1995) 1.
- [36] S.Y. Shiryaev, E.V. Pedersen, F. Jensen, J.W. Petersen, J.L. Hansen, A.N. Larsen, Thin Solid Films 294 (1997) 311.
- [37] C. Teichert, C. Hofer, K. Lyutovich, M. Bauer, E. Kasper, Thin Solid Films 380 (2000) 25.
- [38] C.L. Zhang, B. Xu, Z.G. Wang, P. Jin, F.A. Zhao, Physica E 25 (2005) 592.